Residual Seismic Capacity of UHPC Columns After Fire Exposure

Bo-Jun Huang – Graduate Student, National Cheng Kung University, Department of Civil Engineering, Tainan City, Taiwan, Email: N66104131@gs.ncku.edu.tw

Chung-Chan Hung (corresponding author) – Professor, National Cheng Kung University, Department of Civil Engineering, Tainan City, Taiwan, Email: cchung@ncku.edu.tw

Abstract

This study experimentally investigated the seismic behavior of Ultra-High-Performance Concrete (UHPC) columns after fire exposure. The experimental program included six concrete column specimens reinforced with high-strength reinforcing bars, comprising of two normal-strength concrete (NSC) columns, two high-strength concrete (HSC) columns, and two UHPC columns containing steel and polypropylene fibers at volume fractions of 1.5% and 1.0%, respectively. One column of each type was subjected to a 2-hour fire exposure according to standard heating conditions, while the remaining columns were used as control specimens and not exposed to fire. To assess the fire effect on the seismic performance, all column specimens were subjected to lateral displacement reversals with a constant axial load. The results showed that the lateral strengths of NSC, HSC, and UHPC columns were reduced by 8.0%, 12.0%, and 6.9%, respectively, after fire exposure. Moreover, the effective stiffnesses degraded by 48%, 55%, and 52%, respectively. While the 2-hour fire exposure had a relatively minor effect on the lateral strength of the concrete columns, it considerably reduced the stiffness of the columns irrespective of the concrete material. The use of steel and polypropylene fibers in UHPC was found to be effective in restraining spalling due to fire exposure.

Keywords: High-strength rebar; high-strength concrete; UHPC; columns; fire exposure; seismic performance.

1. Introduction

In recent years, there have been significant developments in the field of high-strength reinforced concrete (HSC) and ultrahigh performance concrete (UHPC), driven by the increasing demand for high-rise buildings and advancements in structural material technology (Kurama and Hung, 2023; Cancan et al., 2022a and 2022b; Hung and Chueh, 2016; Hung and Yen, 2021; Hung and Hung, 2020; Hung et al., 2020, 2022; Manuel et al., 2022; Yi et al., 2021a and 2021b). UHPC, in particular, is characterized by its ultrahigh strength, ductility, and durability under tension and compression, which has motivated experts and researchers to explore its use in various applications (Hung et al., 2021). HSC is known for its denser particle packing density, higher cement content, and lower permeability compared to normal-strength concrete. However, when subjected to fire, these properties can cause HSC to retain the water vapor pressure generated by high-temperature gasification of water molecules, leading to explosive spalling of the concrete without warning. Kodur et al. (2003) suggest that the appropriate ratio of polypropylene fibers in high-strength concrete can effectively reduce explosive spalling. In contrast, lower-strength concrete slowly spalls on the concrete surface. Evaluating the residual structural performance of fire-damaged reinforced concrete structures requires the assessment of cross-sectional isotherm distribution, which is an important indicator. The Eurocode provides the 500°C (932°F) isotherm method, which assumes that concrete outside the 500°C isotherm is ineffective, while concrete within the 500°C isotherm is complete and provides the original strength. This method can be used to evaluate the seismic capacity of reinforced concrete structures after fire damage.

Although there has been extensive research on HSC and UHPC, our understanding of how these materials perform after fire damage remains incomplete. This is particularly concerning as fire, along with earthquakes, remains a leading cause of building damage. Thus, the purpose of this study was to investigate the residual seismic capacity of HSC and UHPC columns after exposure to fire. The study included a 2-hour fire exposure test and cyclic loading test. The residual seismic capacities of the columns were compared in terms of the residual strength and stiffness and failure pattern.

2. Experimental Program

Figure 1 illustrates the design and preparation of six column specimens, which were categorized into three groups based on the type of concrete used: normal-strength concrete (NSC, specimens N35 and F35) with a design strength of 35 MPa (5 ksi), high-strength concrete (HSC, specimens N70 and F70) with a design strength of 70 MPa (10 ksi), and ultrahigh performance concrete (UHPC, specimens N120 and F120) with a design strength of 120 MPa (17.4 ksi). The UHPC contained steel and polypropylene fibers at volume fractions of 1.5% and 1.0%, respectively. All columns had identical designs, except for the type of concrete. They had a section size of 40×40 cm (15.7×15.7 in.) with a cover thickness of 4 cm (1.57 in.) and a clear span of 120 cm (3.94 ft). The columns were reinforced with 8-#8 longitudinal deformed steel bars with a specified yield strength of 550 MPa (80 ksi) and #4 transverse reinforcement with a specified yield strength of 790 MPa (115 ksi) spaced at 6.5 cm (2.56 in.). One specimen from each group (F series) underwent a 2-hour fire exposure test, while the other one (N series) served as a control specimen with no fire exposure. To assess the temperature gradient in the fired specimens (F series) during the tests, thermocouples were installed in accordance with Figure 1(c).

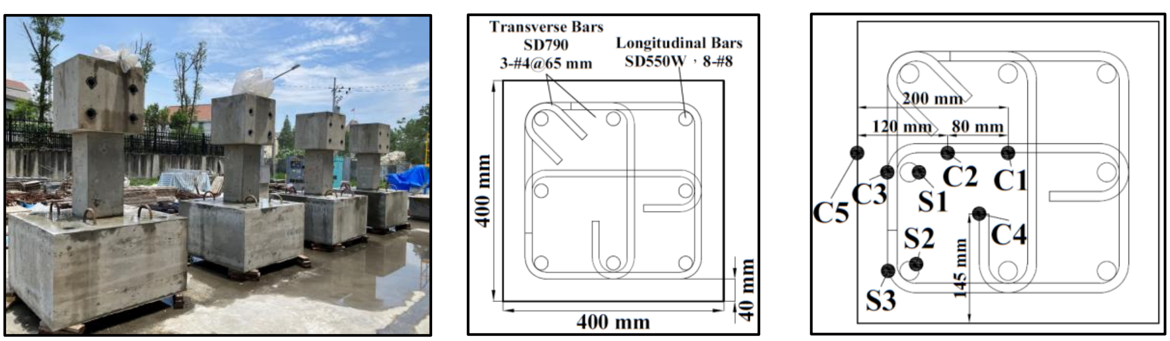

(a) Specimens (b) Cross-sectional design (c) Deployment of thermocouples

Figure 1 Test columns

The specimens subjected to fire exposure (F35, F70, and F120) were placed in a refractory furnace and exposed to a 2-hour standard fire test in accordance with the ISO834-1 heating curve.

The furnace was heated uniformly using liquid petroleum gas, and no axial force was applied during the test. Once the fire test was completed, the specimens were removed from the furnace and allowed to cool naturally until they reached room temperature. To protect the upper and lower bases of the specimens from damage during the fire test, two layers of ceramic fiber fireproof cotton with a total thickness of 7.5 cm (2.95 in.) were applied to their surface prior to the experiment. To avoid insulation effects on the plastic hinge regions of the columns, no fireproof cotton was placed near the columns.

Cyclic loading tests were conducted to assess the seismic behavior of the specimens. The tests began by applying a vertical load equal to a 15% axial load ratio. Next, the columns were subjected to lateral displacement reversals using displacement control. The target drift ratios were set at 0.25%, 0.375%, 0.5%, 0.75%, 1%, 1.5%, 2%, 3%, 4%, 5%, 6%, 7%, and 8%, respectively. Each drift ratio was applied for two cycles.

3. Results and Discussion

3.1. 2-hour Fire Exposure Test

Figure 2 shows the condition of the columns after exposure to fire. The color of the concrete surface changed from gray to yellowish-brown as a result of fire exposure, and craze cracks developed on the columns, which were due to concrete shrinkage resulting from moisture loss. During the tests, significant explosive spalling was observed in F70, which suffered the most damage due to fire exposure. The stirrups in F70 were exposed, indicating that the spalling depth exceeded the cover thickness of 4 cm (1.57 in.). In contrast, relatively minor spalling occurred in F35 and F120, particularly F35. This suggests that HSC is more susceptible to fire exposure than NSC and UHPC with a combined steel and PP fibers.

(a) F35 (b) F70 (c) F120

Figure 2 The status of the columns after fire exposure (east and north sides)

Figure 3 presents the temperature readings obtained by the thermocouples at different locations in the columns during the fire tests, and the measurements were taken for up to four hours after the tests. The temperature gradient of the cross-section was then calculated using linear interpolation, as shown in Figure 4. It was assumed that the columns had isotherms symmetrically distributed along their centerline, and only a quarter of the cross-section is illustrated. The temperature isotherms in F70 were observed to be deeper than those in F35, indicating that the HSC section had a generally higher temperature than the NSC columns. In F120, the depths of the

700°C and 600°C isotherms were deeper than those in NSC and HSC columns. However, the depth of the 500°C and 400°C isotherms in F120 was comparable to N35 and shallower than F70, which explains why the UHPC column remained more intact than the HSC column after fire exposure.

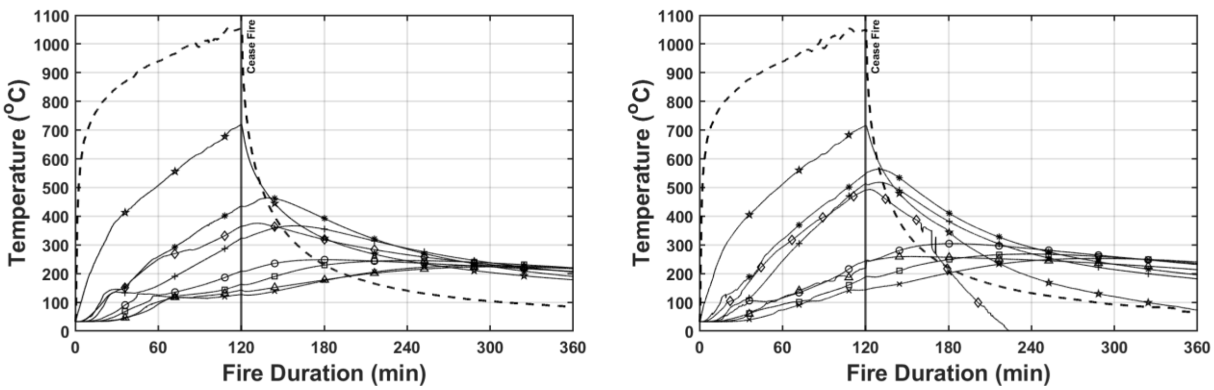

(a) F35 (b) F70

(c) F120

Figure 3 Representative heating curve of fired specimens

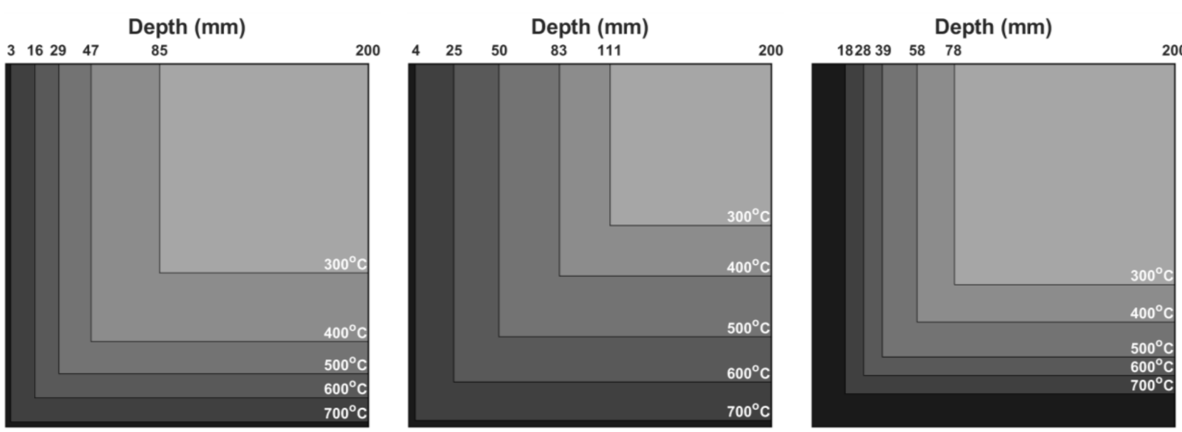

(a) F35 specimen (b) F70 specimen (c) F120 specimen

Figure 4 Each 100°C isotherm of fired specimen on a quarter section

3.2. Cyclic Loading Test

The failure pattern of the column specimens is shown in Figure 5. Figure 6 displays the load-displacement responses. For N35, flexural cracks were dominant until the drift ratio reached 0.75%. When the drift demand exceeded 0.75%, flexural-shear cracks developed. At the plastic hinge regions, concrete crushing occurred at the drift ratios of 2% and 4% in the positive and negative directions, respectively. The maximum lateral strengths in positive and negative directions were 405 kN (91.0 kip) and 397 kN (89.2 kip), respectively, which occurred at the drift ratios of 2.1% and 2.6%, respectively. The effective stiffnesses in positive and negative directions were 30.5 kN/mm (174 kip/in.) and 23.7 kN/mm (135 kip/in.), respectively. For F35, only minor new cracks developed under cyclic loading. Most of the cracks were along existing ones caused by the fire exposure. Concrete crushing occurred at the drift ratios of 5% and 4% in positive and negative directions, respectively. The maximum lateral strengths in positive and negative directions were 359 kN (80.7 kip) and 378 kN (85.0 kip), respectively, which occurred at the drift ratios of 3.7% and 4.7%, respectively. The effective stiffnesses in positive and negative directions were 14.2 kN/mm (81.1 kip/in.) and 13.9 kN/mm (79.4 kip/in.), respectively. It is noteworthy that only minor strength degradation occurred to F35 until the end of the test.

For the N70 specimen, the damage pattern prior to 0.75% drift was dominated by flexural cracks, similar to N35. Flexural-shear cracks gradually developed after 0.75% drift, and concrete crushing occurred more significantly in N70 than in N35. F70 showed a flexural-dominant behavior until the end of the test, and when subjected to lateral displacement reversals, no new cracks or concrete crushing were observed. F70 exhibited only minor strength degradation after the peak strength was reached, which is noteworthy considering the significant damage caused by the fire exposure. The maximum lateral strengths in positive and negative directions for N70 were higher than those for N35. However, while the effective stiffnesses for N70 were higher in the positive direction, it was lower in the negative direction than those for N35. The maximum lateral strength for F70 was lower than that for N70, but still higher than that for F35. The effective stiffnesses for F70 were also lower than those for N70 in both directions, at 16.2 kN/mm (92.5 kip/in.) and 16.1 kN/mm (91.9 kip/in.), respectively, compared to 38.4 kN/mm (219 kip/in.) and 33.1 kN/mm (189 kip/in.), respectively.

For the UHPC column without fire exposure (N120), the damage pattern was dominated by flexural cracks until the drift reached 1%, followed by the gradual development of flexural-shear cracks when the drift exceeded 1.5%. Unlike the NSC and HSC columns, concrete crushing and spalling were not observed during the test, thanks to the bridging effect provided by the steel and PP fibers, which resulted in more and narrower cracks. While the cracks propagated throughout the column height, there were negligible cracks at the bottom of the column due to slight rocking behavior caused by concrete crushing at the interface between the foundation and the UHPC column. The maximum lateral strengths in positive and negative directions were 558 and 599 kN (125 and 135 kip), respectively, occurring at the drift ratios of 2.5% and 4.3%, respectively. The effective stiffnesses in positive and negative directions were 37.7 and 41.1 kN/mm (215 and 235 kip/in.), respectively. The cyclic behavior of N120 was mainly controlled by flexure, with the post-peak strength well sustained until the test ended at 6% drift. When the fired UHPC column was subjected to displacement reversals (F120), only a few new cracks occurred, which developed along the existing cracks caused by the fire exposure. Moreover, there was only minor concrete crushing until the test's end. The cyclic behavior of F120 was flexure-controlled, with the maximum lateral strengths in positive and negative directions of 491 and 586 kN (110 and 132 kip), respectively. The effective stiffnesses in positive and negative directions were 18.9 and 18.7 kN/mm (108 and 107 kip/in.), respectively. In comparison to N120, the effective stiffness in both positive and negative directions of F120 was lower, indicating more significant strength degradation. However, F120 still exhibited satisfactory performance, given that there was only minor concrete crushing and spalling. Compared to the HSC columns (N35 and N70), the UHPC column (N120) showed higher lateral strengths in both positive and negative directions, which can be attributed to its superior material properties and the absence of concrete crushing and spalling. Additionally, the UHPC column (N120) exhibited more and narrower cracks than the HSC columns.

N35 N70 N120 F35 F70 F120

(a) without fire exposure (N series) (b) with fire exposure (F series)

Figure 5 Failure patterns of the test columns after cyclic loading

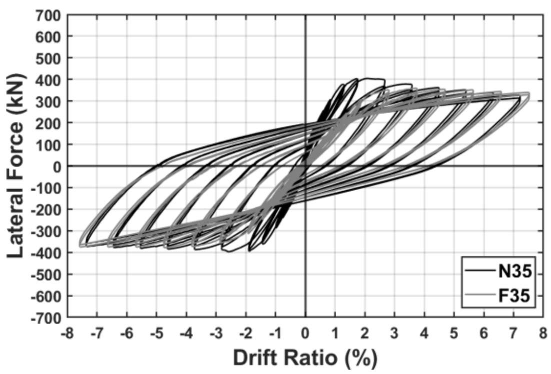

(a) NSC specimens

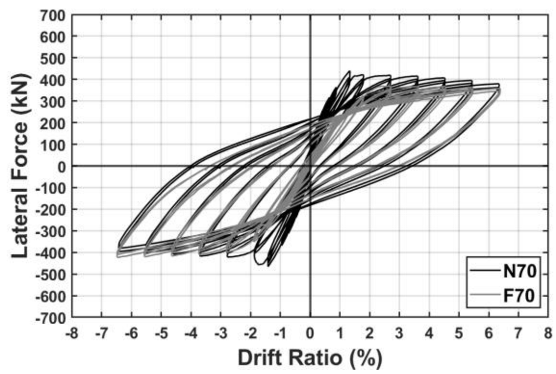

(b) HSC specimens

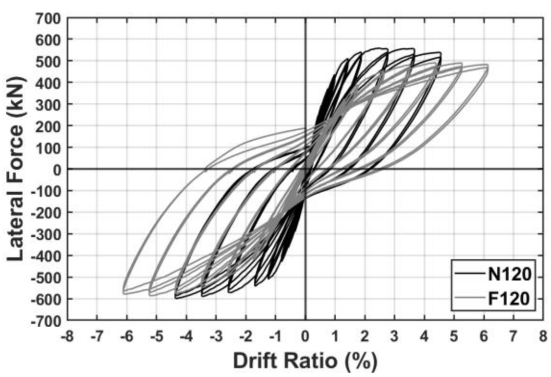

(c) UHPC specimens

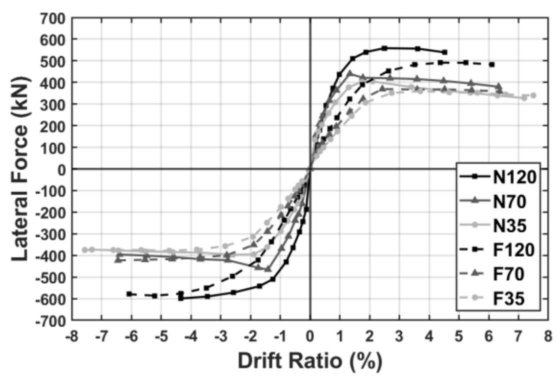

(d) Envelopes

Figure 6 Hysteresis loops

Figure 6(d) compares the strength envelopes of the test specimens. It can be observed that all specimens exhibited flexural-dominant behavior with stable post-peak behavior, indicating that the shear strength of the columns was sufficient and did not significantly degrade due to fire exposure. Furthermore, none of the specimens showed any significant strength degradation, especially for the fire-exposed ones. This is possibly due to the fact that the cover concrete had already spalled and crushed during the fire exposure. As a result, the whole plastic hinge region of the column was well-confined during the displacement reversals. The peak strength of NSC, HSC, and UHPC columns decreased by 8.0, 12.0, and 6.9%, respectively, due to fire exposure. Additionally, the effective stiffness of the columns was reduced by 48, 55, and 52%, respectively. It was observed that while the fire exposure only marginally decreased the lateral strength of the columns, it considerably reduced the stiffness of the columns, irrespective of the type of concrete used, due to the loss of the cover concrete.

Overall, the use of steel and PP fibers in UHPC effectively restrained concrete spalling, providing better post-fire structural performance than NSC and HSC columns. The UHPC column also had a higher ratio of residual strength to original strength than the other columns, given to its combined use of steel and PP fibers.

4. Conclusions

Six concrete column specimens were tested under lateral displacement reversals. The experimental variables included fire exposure and types of concrete (NSC, HSC, and UHPC with combined steel and PP fibers). The test results showed that the HSC column was more susceptible to concrete spalling when exposed to fire. In addition, a higher temperature was in the core region of the HSC column due to its denser microstructure than NSC and significant spalling. Compared to the HSC column, the combined use of steel and PP fibers in the UHPC column effectively reduced the spalling of cover concrete, owing to the bridging effect of fibers and the formation of microchannels due to the melting of PP fibers. During the lateral displacement reversals, all unfired specimens exhibited flexural-dominant behavior. The plastic hinge region of the unfired NSC and HSC columns experienced concrete crushing, which was restrained in the UHPC column. When the fired columns were subjected to cyclic loading, only a few new flexural cracks developed in the NSC column, and new cracks were barely observed in the HSC and UHPC columns. Notably, these new cracks primarily developed along the existing cracks caused by fire exposure. Furthermore, regardless of the type of concrete used, no significant concrete crushing was observed in the fired columns during the displacement reversals. Due to the cover spalling of the fired columns, the degradation of the post-peak strength caused by cyclic loading was minor. However, while the fire exposure only slightly reduced the lateral strength of the columns by about 10%, it considerably reduced the stiffness of the columns by about 50% regardless of the type of concrete materials due to the loss of the cover concrete.

5. References

- Yang, C., Chen, S. C., Yen, C. H., and Hung, C. C., "Behaviour and detailing of coupling beams with high-strength materials." Journal of Building Engineering 47 (2022a): 103843.

- Yang, C., Chou, Y. C., and Hung, C. C., "Seismic behavior of full-scale wall piers with high-strength steel reinforcement." Engineering Structures 256 (2022b): 114068.

- Hung, C. C., and Chueh, C. Y. "Cyclic behavior of UHPFRC flexural members reinforced with high-strength steel rebar." Engineering Structures 122 (2016): 108-120.

- Hung, C. C., and Yen, C. H., "Compressive behavior and strength model of reinforced UHPC short columns." Journal of Building Engineering 35 (2021): 102103.

- Hung, C. C., and Hung, H. H., "Potential of sodium sulfate solution for promoting the crack-healing performance for strain-hardening cementitious composites." Cement and Concrete Composites 106 (2020): 103461.

- Hung, C. C., El-Tawil, S., and Chao, S. H., "A review of developments and challenges for UHPC in structural engineering: Behavior, analysis, and design." Journal of Structural Engineering 147.9 (2021): 03121001.

- Hung, C. C., Yuen, T. Y., Huang, C. W., and Yen, C. H., "Tension lap splices in piers UHPC beams: Influence of rebar size, steel fibers, splice length, and coarse aggregate." Journal of Building Engineering 55 (2022): 104716.

- Hung, C. C., Chen, Y. T., & Yen, C. H., "Workability, fiber distribution, and mechanical properties of UHPC with hooked end steel macro-fibers." Construction and Building Materials 260 (2020): 119944.

- European Committee, "Eurocode2: Design of concrete structures-Part1-2: General rules-Structural fire design," EN 1992-1-2:2004:E, 2004.

- Bermudez, M., Wen, K. W., and Hung, C. C., "A comparative study on the shear behavior of UHPC beams with macro hooked-end steel fibers and PVA fibers." Materials 15.4 (2022): 1485.

- Kodur, V. K. R., et al. "Effect of strength and fiber reinforcement on fire resistance of high-strength concrete columns." Journal of Structural Engineering 129.2 (2003): 253-259.

- Kurama, Y. C., and Hung, C. C., "RC Structures with High and Ultrahigh-Performance Materials." (2023): 02022003.

- Shao, Y., Kuo, C. W., and Hung, C. C., "Seismic performance of full-scale UHPC-jacket-strengthened RC columns under high axial loads." Engineering Structures 243 (2021a): 112657.

- Shao, Y., Hung, C. C., and Billington, S. L. "Gradual crushing of steel reinforced HPFRCC beams: Experiments and simulations." Journal of Structural Engineering 147.8 (2021b): 04021114.